Surface-mediated light transmission in metal nanoparticle chains

P. Jasper Compaijen, Victor A. Malyshev, and Jasper Knoester*
Center for Theoretical Physics and Zernike Institute for Advanced Materials, University of Groningen, Nijenborgh 4, 9747 AG Groningen, The Netherlands
(Received 16 April 2013; revised manuscript received 10 May 2013; published 28 May 2013)

We study theoretically the efficiency of the transmission of optical signals through a linear chain consisting of identical and equidistantly spaced silver metal nanoparticles. Two situations are compared: the transmission efficiency through an isolated chain and through a chain in close proximity of a reflecting substrate. The Ohmic and radiative losses in each nanoparticle strongly affect the transmission efficiency of an isolated chain and suppress it to large extent. It is shown that the presence of a reflecting interface may enhance the guiding properties of the array. The reason for this is the energy exchange between the surface plasmon polaritons (SPPs) of the array and the substrate. We focus on the dependence of the transmission efficiency on the frequency and polarization of the incoming light, as well as on the influence of the array-interface spacing. Sometimes the effect of these parameters turns out to be counterintuitive, reflecting a complicated interplay of several transmission channels.

DOI: 10.1103/PhysRevB.87.205437 PACS number(s): 73.21.−b, 73.20.Mf, 78.67.Sc

I. INTRODUCTION

Metal nanoparticles (MNPs) are known to have scattering cross-sections that can exceed the MNP's geometrical cross-section by more than an order of magnitude, if the excitation is close to the localized surface plasmon resonance of the particle.[1,2] This property makes MNPs attractive building blocks for nano-optics. The strong near-field enhancement and light scattering of the nanoparticles have led to a number of interesting applications in spectroscopy[3] and nanoantennas.[4–8] An important application, which will be the focus of this paper, is the possibility to guide and propagate an optical excitation through a chain of metal nanoparticles. This application was first proposed by Quinten *et al.*[9] in 1998, and since then this system has attracted a great deal of attention. Guiding, bending, splitting,[10–13] and localization[14,15] of the optical excitations of the chain, as well as the time dependent properties,[16] have been studied carefully. Important insight into guiding properties of these systems was gained after computing the dispersion relations,[10,17–22] both for finite and infinite chains. From these studies, it became clear that far-field interactions are very important[17] and that the excitations in the chain are of a surface plasmon polariton (SPP) nature.[18]

It is well known that the radiative properties of emitters change if their local environment is modified. The lifetime of a molecule in the proximity of a metal or dielectric substrate can change drastically, depending on its orientation and distance to the substrate.[23–25] Similarly, one can expect changes in the guiding properties of the MNP chain. For small enough array-substrate spacings, not only the radiative but also the nonradiative decay properties will be altered.[26] It has been shown that under some conditions, SPP modes on the interface of the substrate can be excited and guided along the array.[27]

In this paper, we modify the local environment of an array of MNPs by positioning the array close to a (partially) reflective substrate. We discuss the effect of the substrate on the guiding properties of the array. Understanding this influence is important: in any nanoscale application or experiment, there will be a reflecting interface in the proximity of the array. From a more fundamental point of view, studying this system is interesting because it allows one to tune the interactions between the MNPs,[28] and, to a certain extent, the radiative losses of the particles. We consider and compare three different cases: an isolated array, an array close to a perfectly reflecting substrate, and an array close to a real substrate (silver, in particular). We study how the array's efficiency to transmit an optical signal depends on the frequency and polarization of the excitation, as well as on the array-substrate spacing. The MNPs are modeled in the point-dipole approximation, making use of a generalized Drude model for their permittivity. The coupling between the MNPs in free space is calculated using the full, retarded Green's tensor for a homogeneous medium. The presence of the interface is taken into account by constructing a Green's tensor for the scattered field, within the framework of Sommerfeld's treatment for the field that is reflected from the interface.

The paper is organized as follows. In the next section, we describe the system setup and the mathematical formalism. In Sec. III, the results of calculations of the transmission efficiency ($\mathcal{T}$) of the array are presented for the three different system choices mentioned above. The dependence of the $\mathcal{T}$ on the excitation polarization, excitation frequency, and on the array-substrate spacing are discussed. Finally, in Sec. IV, we summarize.

II. SYSTEM SETUP AND FORMALISM

We consider a linear array of N identical spherical nanoparticles, embedded in a medium with permittivity ϵ_1, positioned parallel and at a distance h from a substrate with permittivity ϵ_2. The nanoparticles have radius a and are equally spaced with center-to-center distance d (see Fig. 1). In the calculations, we treat each MNP as a point dipole and describe the interaction between the particles using the retarded dipole-dipole interactions. The point-dipole approximation is accurate if the variation of the field over the particle is small ($a \ll \lambda$, λ being the excitation wavelength), and the inequality $d > 3a$ holds.[29] We assume a continuous wave (cw) excitation of only the leftmost particle.

The amplitude of the dipole moment $\mathbf{p}$ induced in an MNP, subject to an electric field of amplitude $\mathbf{E}$, can be characterized

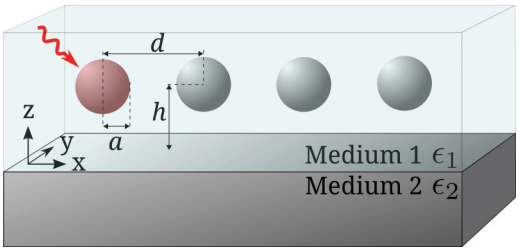

FIG. 1. (Color online) Schematics of the system under consideration: a linear array of identical and equidistantly spaced spherical MNPs with radius a and center-to-center distance d. The array is embedded in a medium with permittivity ϵ_1 and located at a distance h from a substrate with permittivity ϵ_2. Only the leftmost particle is considered to be excited. The x axis is parallel to the array and the z axis is perpendicular to the interface.

by the frequency dependent MNP polarizability $\alpha(\omega)$,

$$\mathbf{p} = \epsilon_1 \alpha \mathbf{E}, \tag{1}$$

where we omitted the argument ω in α for the sake of simplicity. Please note that also the time dependence is removed from the above equation, we will focus on the amplitudes of steady-state solutions only. In the point-dipole approximation, α is given by

$$\frac{1}{\alpha} = \frac{1}{\alpha^{(0)}} - \frac{k_1^2}{r} - \frac{2i}{3}k_1^3. \tag{2}$$

Here, $\alpha^{(0)}$ is the so-called bare polarizability, which can be derived from electrostatics, and $k_1 = (\omega/c)\sqrt{\epsilon_1}$ is the wave vector of light in the host medium. The k_1-dependent terms are corrections due to the depolarization field generated inside the nanosphere.[30] The k_1^2 term describes the spatial dispersion correction, whereas the k_1^3 term accounts for radiation damping. For particles with radii of a few tens of nanometers, it is sufficient to use just these first two corrections, so higher order terms can be safely neglected. In the quasistatic approximation ($a \ll \lambda$), the bare polarizability reads[1,31]

$$\alpha^{(0)}(\omega) = \frac{\epsilon(\omega) - \epsilon_1}{\epsilon(\omega) + 2\epsilon_1} a^3, \tag{3}$$

where $\epsilon(\omega)$ indicates the permittivity of the bulk metal. Note that ϵ strongly depends on the frequency ω and can be negative in a certain frequency range. The poles of $\alpha^{(0)}(\omega)$, i.e., the solutions to the equation $\mathrm{Re}(\epsilon) = -2\epsilon_1$, correspond to the localized surface plasmon resonance (see, e.g., Ref. 2).

In a chain, the MNPs will couple to each other due to electromagnetic interactions. The electromagnetic field produced by an oscillating dipole embedded in a homogeneous medium, can be written in the terms of the Green's tensor of a homogeneous medium. In Cartesian coordinates, this tensor is given by[32]

$$\overleftrightarrow{\mathbf{G}}^H(\mathbf{r},\mathbf{r}_0) = \frac{e^{ik_1R}}{R}\left[\left(1 + \frac{ik_1R - 1}{k_1^2R^2}\right)\overleftrightarrow{\mathbf{I}} + \frac{3 - 3ik_1R - k_1^2R^2}{k_1^2R^2}\frac{\mathbf{RR}}{R^2}\right]. \tag{4}$$

In this equation, R represents the distance from the source $\mathbf{r}_0$ to the detection point $\mathbf{r}$. The corresponding electric field is $\mathbf{E} = \epsilon_1^{-1}k_1^2\overleftrightarrow{\mathbf{G}}^H(\mathbf{r},\mathbf{r}_0)\mathbf{p}$. To account for the presence of a substrate, we introduce a Green's tensor $\overleftrightarrow{\mathbf{G}}^S$ that describes the field reflected from the interface. To do this, we make use of the work done by Sommerfeld on radio antennas close to the earth, which can be directly applied to radiating dipole positioned close to an interface. There is extensive literature about this method.[33,34] As an example, we will only present the zz component of $\overleftrightarrow{\mathbf{G}}^S$ (see Fig. 1 for the definition of the x, y, and z directions):

$$G^S_{zz}(\mathbf{r},\mathbf{r}_0) = \left[1 + \frac{ik_1R' - 1}{k_1^2R'^2} + \frac{3 - 3ik_1R' - k_1^2R'^2}{k_1^2R'^2}\frac{(z+h)^2}{R'^2}\right]\frac{e^{ikR'}}{R'} - \frac{2i}{k_1^2}\int_0^\infty J_0(k_\rho\rho)\frac{k_\rho^3}{k_{1z}}\frac{\epsilon_1 k_{2,z}}{\epsilon_1 k_{2z} + \epsilon_2 k_{1z}}e^{ik_{1z}(z+h)}dk_\rho. \tag{5}$$

This equation gives the z component of the electric field in medium 1 produced by a z-polarized oscillating dipole in the same medium, located at a height h above the interface with medium 2. R' is the distance from the image dipole in medium 2 to the detection point $\mathbf{r}$, i.e., $R' = [x^2 + y^2 + (z+h)^2]^{1/2}$, $\rho = (x^2 + y^2)^{1/2}$, k_i denotes the wave number in medium i, $k_\rho = (k_x^2 + k_y^2)^{1/2}$ is the in-plane wave vector, and $k_{iz} = (k_i^2 - k_\rho)^{1/2}$, is the component of the wave vector perpendicular to the interface in medium i. The function J_0 is the zeroth order Bessel function. The integrals of $\overleftrightarrow{\mathbf{G}}^S$ are evaluated along an appropriate integration path using a Gauss-Kronrod quadrature. A detailed description of this method is given in Ref. 34.

From comparison of Eqs. (4) and (5), it becomes clear that the first part of Eq. (5) represents the field produced by a free space dipole located at $z = -h$ (image dipole, see for illustration Fig. 2), and therefore, it can be identified as the field scattered by a perfectly reflecting interface. In the case of a perfect reflector, we have $\epsilon_2 \to \infty$, so that, indeed, the second term in Eq. (5) will vanish. Thus the integral in Eq. (5) can be interpreted as a correction to a perfect reflector, and includes effects coming from the excitation of surface modes. For $k_\rho < k_1$, the reflected waves are propagating away from the interface into medium 1, whereas for $k_\rho > k_1$, the z component of the wave vector $k_{1,z}$ is imaginary and therefore these waves will be surface waves, bound to the interface. A special type of surface wave, SPP, occurs when k_ρ is such that the denominator $\epsilon_1 k_{2z} + \epsilon_2 k_{1z} = 0$, i.e., $k_\rho = k_0(\epsilon_1\epsilon_2/(\epsilon_1 + \epsilon_2))^{1/2}$. In the case of an interface between a metal and a dielectric, the conditions $\epsilon_1\epsilon_2 < 0$ and $|\epsilon_2| > |\epsilon_1|$ can be satisfied, which implies that

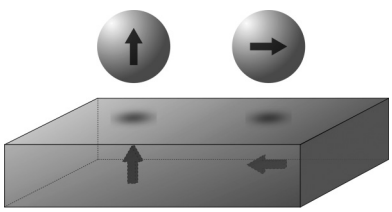

FIG. 2. Illustration of the orientation of the induced image dipoles. For a dipole polarized perpendicular to the interface, the image dipole will have the same polarization. For a dipole polarized parallel to the interface, the image dipole will have antiparallel polarization.

k_ρ is real and k_{iz} is imaginary, i.e., the mode propagates along the interface and is bound to it.

With this knowledge in mind, we can set up a system of coupled equations for the dipole moment $\mathbf{p}_m$ of each particle m as

$$\frac{1}{\epsilon_1}\sum_m \left[\frac{1}{\alpha}\delta_{nm}\overleftrightarrow{\mathbf{I}} - k_1^2(\overleftrightarrow{\mathbf{G}}^H(\mathbf{r}_n,\mathbf{r}_m)+\overleftrightarrow{\mathbf{G}}^S(\mathbf{r}_n,\mathbf{r}_m))\right]\mathbf{p}_m = \mathbf{E}_n. \tag{6}$$

Here, $\overleftrightarrow{\mathbf{G}}^H(\mathbf{r}_n,\mathbf{r}_n)$ should be taken equal to zero.[35] Using this equation, the dipole moment of each particle can be calculated for a given input electric field of amplitude $\mathbf{E}_0$.

III. RESULTS AND DISCUSSION

In this section, we present and discuss the transmission of optical excitations through a chain of 20 silver nanospheres, choosing a particular set of parameters: radius $a = 25$ nm, center-to-center distance $d = 75$ nm, and distance from the chain axis to the substrate $h = 50$ nm. The point-dipole approximation for this particular parameters has been verified using a boundary element method (BEM) calculation[36] and the validity of this approximation with respect to energy conservation is carefully studied in Ref. 37. To quantify the transmission, we calculate the transmission efficiency $\mathcal{T}$, which we define as the ratio of the modulus squared of the dipole moments of the rightmost (last) to the leftmost (first) particle,

$$\mathcal{T} = \frac{||\mathbf{p}_N||^2}{||\mathbf{p}_1||^2}. \tag{7}$$

Remember that only the leftmost MNP is driven by the incoming field. The permittivity of the silver MNPs and substrate is described with a generalized Drude model:

$$\epsilon(\omega) = 5.45 - 0.73\frac{\omega_p^2}{\omega^2 + i\omega\gamma}, \tag{8}$$

where $\omega_p = 17.2$ fs^{-1} and $\gamma = 0.0835$ fs^{-1}. Equation (8) provides a good fit to experimental data in the relevant frequency region.[38] Three different geometries of the system will be considered: an isolated chain, a chain in the proximity of a perfect reflector, and a chain close to a silver substrate. We also are interested in different excitation geometries: x, y, and z polarized. The results obtained for the $\mathcal{T}$ at a fixed array-substrate separation are presented in Fig. 3 as a function of the wavelength in medium 1.

A. Isolated chain

First, we consider the $\mathcal{T}$ of an isolated chain for different excitation polarizations (dashed-dotted curves in all panels of Fig. 3). As is seen, the $\mathcal{T}$s for y- and z-polarized excitations (transversal) are equal to each other, whereas in both cases the $\mathcal{T}$ is much lower than that for x polarization (longitudinal). The reason for this is that for an interparticle separation of 75 nm, near-field interactions are dominant. This interaction is twice as large for longitudinally oriented dipoles as compared to transversally oriented ones, which gives rise to a higher $\mathcal{T}$. For dipoles oriented longitudinal to the chain axis, the radiation is directed outward of the chain. For long excitation wavelengths, more of these dipoles will be oscillating in phase,[17] and therefore more energy will be radiated out, instead of transmitted along the array. This explains the absence of the long-wavelength tail, which is seen for transverse excitation. This tail originates from the asymmetry of the polarizability of a single MNP.

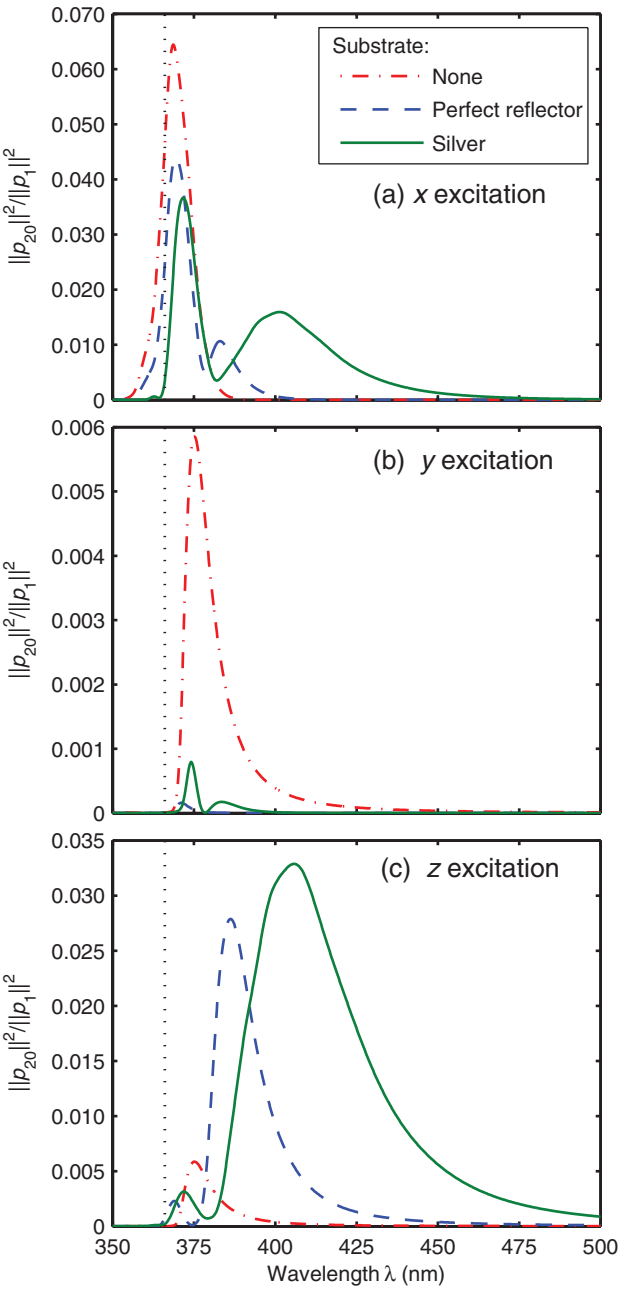

FIG. 3. (Color online) Transmission efficiency $\mathcal{T}$, Eq. (7), for a chain of 20 identical spherical silver MNPs (radius $a = 25$ nm, center-to-center distance $d = 75$ nm) for three different systems: in red (dashed-dotted)is an isolated chain, in blue (dashed) is a chain above a perfectly reflecting substrate (height $h = 50$ nm), and in green (solid) is a chain above a silver substrate (height $h = 50$ nm). The polarization of the excitation is denoted in the legend. The black vertical dotted line indicates the plasmon resonance of a single particle (366 nm).

Although in the rest of this paper we limit our discussion to a chain of $N = 20$ particles and an interparticle spacing of $d = 75$ nm, the effects of changing these parameters can be easily

argued from understanding the properties of retarded dipole-dipole interactions. Increasing d will reduce the interparticle coupling strength and, as a result, decrease $\mathcal{T}$. The coupling of dipoles with a polarization perpendicular to the chain (y or z) contains terms depending on R^{-1}, R^{-2}, and R^{-3}, whereas for dipoles with a polarization parallel to the chain (x) this only contains the R^{-2} and R^{-3} terms. Therefore the decrease in $\mathcal{T}$ will be stronger for parallel polarization. Adding more particles to the chain, while leaving d unchanged, implies adding more loss channels (both radiative and Ohmic), and therefore will decrease the signal at the last particle.

The $\mathcal{T}$ relates the dipole moment of the last particle of the chain to the first. Thus increasing the number of particles, while keeping the interparticle spacing unchanged, will give rise to a lower $\mathcal{T}$, because more losses are introduced in the chain.

The position of the $\mathcal{T}$ maximum can be explained by calculating the dispersion relations of the system. As discussed in Ref. 18, the mode with the longest propagation length is expected to be the mode for which the product of group velocity and the lifetime is maximized. The frequency of this mode corresponds exactly to the $\mathcal{T}$ maximum. For an isolated chain, there is one mode dominating the $\mathcal{T}$, but this is not necessarily the case for a chain over a reflector, as we will see below.

B. Perfect reflector versus nonperfect reflector

When considering the signal transmission through a chain in the proximity of a reflector, it is worth noting that the presence of a reflecting interface not necessarily enhances the $\mathcal{T}$ of the chain. In particular, when the MNPs have a polarization parallel to the interface, the $\mathcal{T}$ decreases as compared to an isolated chain of the same length. The reason is that the dipole moment of an MNP, together with its image, forms an effective quadrupole (see Fig. 2, right), thus reducing the effective electromagnetic interaction between neighboring MNPs. In the case of z excitation, the dipole moment of an MNP and its image forms an enlarged dipole (see Fig. 2, left), which leads to a stronger coupling between the MNPs, and, as a result, in an increased $\mathcal{T}$ as compared to an isolated chain. For both parallel and perpendicular polarization, the interaction with the image gives rise to a redshift of the MNP's plasmon resonance. A detailed study of these effects for a single MNP can be found in Ref. 39.

The $\mathcal{T}$ spectra for a chain over a perfectly reflecting substrate (dashed curves in Fig. 3) show two peaks for x- and z-polarized excitation, instead of a single one, as in the case of an isolated chain [see Figs. 3(a) and 3(c)]. Inspecting the directivity of dipole radiation reveals that due to the presence of a reflector, a z-polarized dipole can excite in the neighboring particle an x-polarized dipole and vise versa (see Fig. 4). Thus, whereas x, y, and z polarizations are completely decoupled for an isolated chain, x and z polarizations now form coupled modes. One of the peaks originates mainly from x-polarized dipoles and the other one results mainly from z-polarized dipoles. This fact is supported by the observation that, in the case of a chain over a perfectly reflecting substrate, the two peaks occur at the same wavelengths for both polarizations. For excitation along the x axis, the left peak is much more intense than the right one, indicating a dominant contribution to the $\mathcal{T}$ of the x-polarized propagating modes. The right (much smaller) peak comes from the interface-mediated coupling to the z-polarized modes. The situation is reversed when the excitation is z polarized.

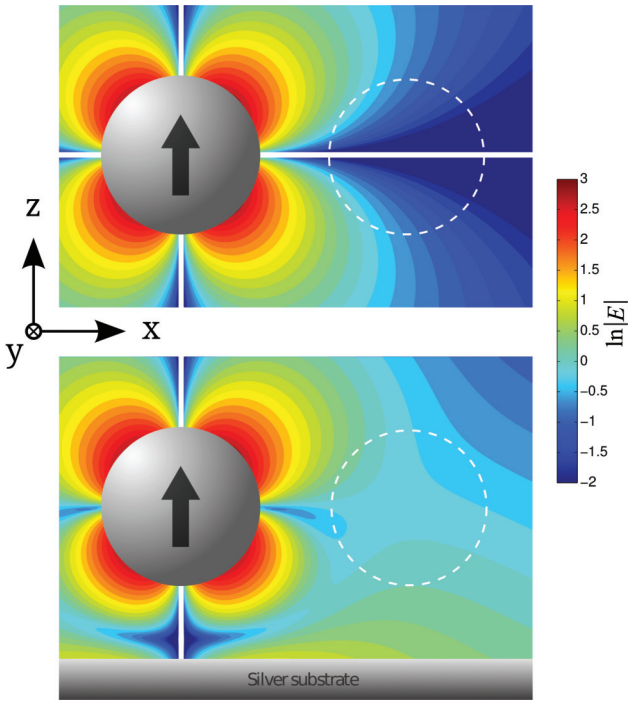

FIG. 4. (Color online) Maps of the x component of the electric field produced by a z-polarized metal nanoparticle. (Top) Isolated particle. (Bottom) Particle located 50 nm above a silver substrate. Dashed circles indicate a neighboring nanoparticle. The lower plot shows that in the presence of a reflecting interface, there will be a coupling between x and z polarizations. In the absence of a reflector, this coupling is identical to zero in the point-dipole model. The above figure shows that this approximation is valid if the particles are small enough and not too closely spaced. Note that the absolute value of the field is plotted on a logarithmic scale. The white stripes correspond to zero electric field.

With or without a reflecting interface, y-polarized dipoles will only excite oscillations of neighboring MNPs with the same polarization. This gives rise to a single peak in the $\mathcal{T}$ for an isolated chain and for a chain over a perfect reflector. The reason for the weak transmission in the case of a perfectly reflecting substrate is that the reflected field has opposite phase as compared to the field coming directly from the MNP. The destructive interference of these two contributions results in a weaker interaction along the chain and therefore in a lower $\mathcal{T}$.

As was noticed in Sec. II, a silver substrate differs from a perfect reflector because not all radiation is reflected from the former; some part of it is transmitted into the silver or excites surface modes, like SPPs. At first glance, it might come as a surprise that the $\mathcal{T}$ of a chain of MNPs close to a nonperfect reflector, like silver, can be higher than in the presence of a perfectly reflecting substrate. The physics of this counterintuitive result can be understood from the coupling of the chain excitations to the SPP modes of the substrate. Due to the fact that these modes are localized on the interface, they give rise to strong fields close to the interface, and can therefore enhance the coupling between

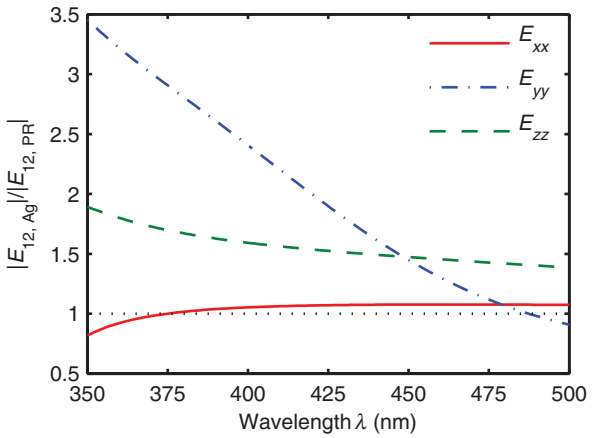

FIG. 5. (Color online) The ratio $|E_{12,\mathrm{Ag}}|/|E_{12,\mathrm{PR}}|$ of the electric field magnitudes produced by the first (1) particle of the chain in the position of the neighboring one (2) for a chain at a height of $h = 50$ nm above a silver substrate (Ag) and above a perfect reflector (PR), as a function of the wavelength for different excitation polarizations. The center-to-center distance between the particles is $d = 75$ nm.

neighboring MNPs. Figure 5 shows the ratio of the electric field magnitudes $|E_{12,Ag}|$ and $|E_{12,PR}|$ produced by the first particle of the chain in the position of the second one for a silver substrate (Ag) and a perfect reflector (PR), respectively, as a function of frequency of wavelength for different excitation polarizations. Note that this shows the relative electric fields, not the actual field strengths. From this figure, it can be clearly seen that over almost the whole range of wavelengths, the field produced in a neighboring MNP above a silver substrate is larger than for the case of a perfectly reflecting substrate. Only for x polarization at small wavelengths the perfect reflector gives rise to a stronger coupling, which explains the slight decrease of the $\mathcal{T}$ for the left peak under x-polarized excitation in the case of the silver substrate [see Fig. 3(a)].

Due to the bound nature of the SPP modes of the substrate, they have a larger wave vector than light of the same frequency has. Therefore, to excite these modes with MNPs, phase-matching conditions dictate that the chain-substrate spacing should be smaller that the actual wavelength, i.e., the substrate should be positioned within the near-field region of the MNP. The reason for this is that the near field of oscillating dipoles contain the required high wave-vector contributions. Since the amplitudes of SPP modes decay exponentially away from the interface, a strong influence of these modes on the $\mathcal{T}$ is only expected for small chain-interface separations. It has been shown that, for the geometry under consideration, SPP modes can be guided over the interface, along a chain of MNPs[27] and that these surface modes can propagate for long distances.[3] In the case of a silver substrate, the transmission of optical signals through the MNP chain will be due to the propagation of collective chain-substrate modes. For substrate-SPP modes, it is well known that the propagation length increases for larger wavelengths,[3] and therefore also an increased $\mathcal{T}$ and a redshift of the transmission maximum is expected. Dipoles oscillating perpendicular to a metal substrate are known to couple stronger to SPP modes than dipoles oriented parallel, because the latter will excite both s- and p-polarized surface waves, whereas the former will only excite surface waves with p polarization of which the SPP is one. Figure 3 shows that in the presence of a silver substrate, the z-polarized peaks of the $\mathcal{T}$ increase and shift to the red, as compared with a perfectly reflecting substrate.

Interestingly, also a broadening of the transmission spectrum is observed. Broadening is often associated with a decreased lifetime, for example, due to the presence of an extra decay channel. In fact, the presence of a silver interface can be considered as a decay source for an MNP, because exciting substrate-SPPs is an extra channel to lose its excitation. Calculation of the effective polarizability of an MNP above a silver substrate, indeed shows a broadening. A broader spectral response of a single MNP will give rise to a broader transmission efficiency as well, which implies that a larger range of frequencies can be transmitted along an array of MNPs. This is interesting from the point of view of applications.

C. Influence of chain-interface separation

For the system under y excitation, one observes in Fig. 3 an interesting difference between the $\mathcal{T}$ spectra for a perfectly reflecting substrate and a (real) silver one: in the latter case, the spectrum has an extra peak. To understand the origin of this peak, we performed a study of the $\mathcal{T}$ dependence on the chain-interface separation h (see Fig. 6). It is seen from Fig. 6(b) that, upon increasing h, the right peak approaches the one for an isolated chain, suggesting that both have the same physical origin. This is not surprising: for larger h, the interactions between the MNPs is much larger than the MNP substrate coupling and dominates the $\mathcal{T}$. The redshift of this peak upon reducing h results from the formation of effective dipole-image quadrupoles. Since this formation leads to weaker electromagnetic forces along the chain, it also reduces the magnitude of the peak.

By contrast, the left peak increases in magnitude upon decreasing h, hinting towards a strong contribution of SPP modes. A careful examination of the peak behavior shows that, for small h, the peak position exactly matches the single-particle plasmon resonance in the presence of the silver substrate. This implies that in this case, the MNP-substrate coupling is much stronger than the interparticle interactions. Therefore the physical origin of the right peak derives from the decay of the plasmon excitation of the leftmost MNP into SPP modes of the substrate; these modes are then guided along the chain and excite the other particles. A detailed study of these SPP-mediated interactions can be found in Ref. 25.

Taking a closer look at the $\mathcal{T}$ spectra for x and z excitations, we see that in this case the silver substrate also gives rise to an additional, small and redshifted peak as compared with a perfect reflector. The main difference between a perfect reflector and a silver substrate in this frequency domain is the possibility to excite surface modes. Therefore these extra peaks can also be attributed to the SPPs contribution. Here, the peak position does not match the single-particle resonance, because the interparticle interaction still is quite strong. Since the transmission can occur both via x- and z-polarized modes, there are several competing channels. The SPP channel is expected to become weaker when increasing the chain-substrate spacing h. However, for x excitation, increasing h also reduces the coupling to z-polarized modes, thereby

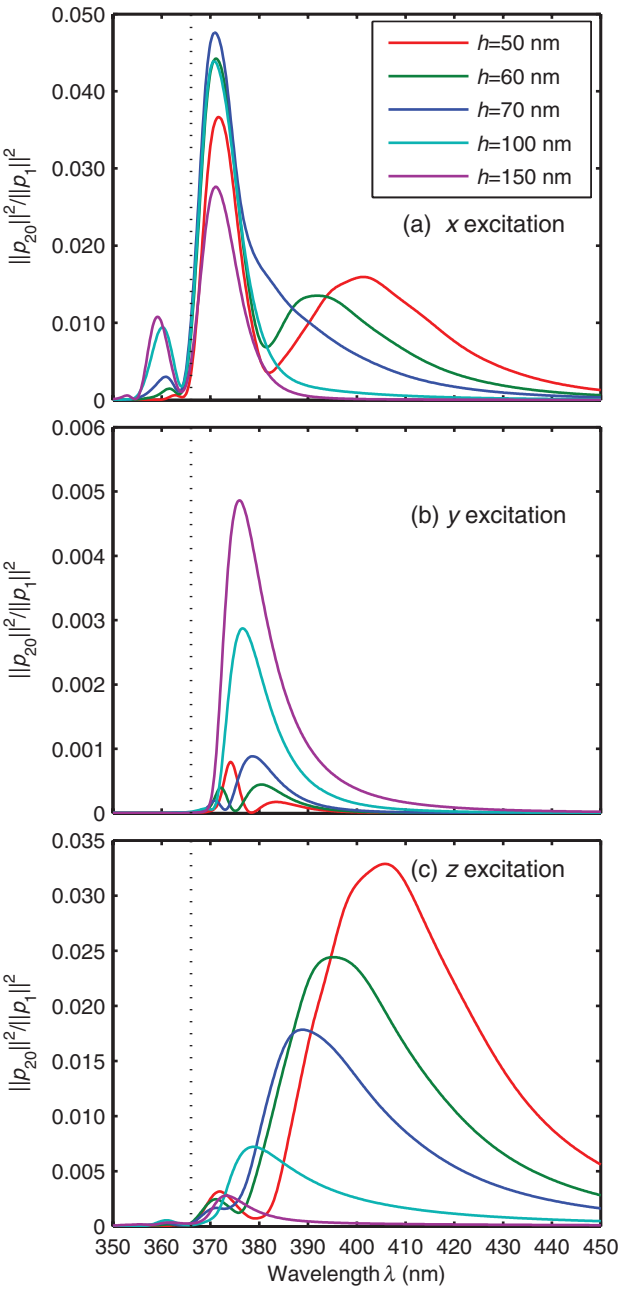

FIG. 6. (Color online) Transmission efficiency for a chain of 20 identical spherical silver MNPs (radius $a = 25$ nm, center-to-center distance $d = 75$ nm) for different heights h above a silver substrate. The values of h are indicated in the figure legend. The black, vertical, dotted line indicates the plasmon resonance of a single particle (366 nm).

lowering the z-polarized $\mathcal{T}$. Because of that, the SPP channel becomes more important. As a result, the corresponding peak grows upon increasing h. Naturally, for even larger spacings, this peak will decrease again, since the coupling to SPPs decays exponentially away from the interface and can only occur if the substrate is within the near-zone region of the MNP field.

IV. SUMMARY AND CONCLUDING REMARKS

We studied theoretically the transmission efficiency of visible light through a linear chain consisting of equidistantly spaced identical silver metal nanoparticles (MNPs) under cw excitation of only the leftmost particle. Three different arrangements of the system were considered: an isolated chain, a chain in proximity to a perfect reflector, and a chain close to a real reflector (silver substrate). We also considered different geometries of excitation: x polarized (along the chain axis), y polarized (perpendicular to the chain axis, parallel to the substrate), and z polarized (perpendicular to the chain axis and the substrate). We found a complicated dependence of the transmission efficiency on the polarization and provided simple explanations of the peculiarities observed, making use of the dipole-image picture and coupling of the MNP chain to SPP modes.

Surprisingly, for z polarization, the silver substrate leads to a much larger transmission efficiency than a perfect reflector, additionally giving rise to a wider spectral range of the transmission. We attribute this effect to the efficient energy exchange between the substrate-SPPs and the chain-SPPs. The former have larger propagation lengths than the latter, and therefore provide better conditions for the light transmission. In the case of x polarization, the transmission efficiencies of both systems are comparable. We also addressed the dependence of the transmission efficiency and its spectrum on the array-interface spacing (for a silver substrate) and found a complicated behavior, depending on the excitation polarization, which, nevertheless, has a transparent physical explanation.

To conclude, we point out that, similar to the case of an isolated chain,[18] the dispersion relation of the collective electromagnetic excitations of the MNP chain in the presence of a reflecting interface is of great importance to further understand the energy exchange between the chain and the substrate and the possibility to guide light below the diffraction limit. This is the topic of ongoing research.

ACKNOWLEDGMENTS

The authors acknowledge J. Munárriz for the BEM calculations to verify the dipole approximation. This work is supported by NanoNextNL, a micro- and nanotechnology consortium of the Government of the Netherlands and 130 partners.

*j.knoester@rug.nl

[1] C. F. Bohren and D. R. Huffman, *Absorption and Scattering of Light by Small Particles* (Wiley, New York, 1983).
[2] S. A. Maier, *Plasmonics: Fundamentals and Applications* (Springer, New York, 2007).
[3] S. A. Maier, Opt. Express **14**, 1957 (2006).
[4] L. Novotny and N. van Hulst, Nature Photon. **5**, 83 (2011).
[5] A. F. Koenderink, Nano Lett. **9**, 4228 (2009).
[6] P. Bharadwaj, B. Deutsch, and L. Novotny, Adv. Opt. Photon. **1**, 438 (2009).

[7]T. Coenen, E. J. R. Vesseur, A. Polman, and A. F. Koenderink, Nano Lett. **11**, 3779 (2011).
[8]J. Munárriz, A. V. Malyshev, V. A. Malyshev, and J. Knoester, Nano Lett. **13**, 444 (2013).
[9]M. Quinten, A. Leitner, J. R. Krenn, and F. R. Aussenegg, Opt. Lett. **23**, 1331 (1998).
[10]M. L. Brongersma, J. W. Hartman, and H. A. Atwater, Phys. Rev. B **62**, R16356 (2000).
[11]D. S. Citrin, Nano Lett. **4**, 1561 (2004).
[12]D. S. Citrin, Nano Lett. **5**, 985 (2005).
[13]B. Willingham and S. Link, Opt. Express **19**, 6450 (2011).
[14]R. de Waele, A. F. Koenderink, and A. Polman, Nano Lett. **7**, 2004 (2007).
[15]A. V. Malyshev, V. A. Malyshev, and J. Knoester, Nano Lett. **8**, 2369 (2008).
[16]S. A. Maier, P. G. Kik, and H. A. Atwater, Phys. Rev. B **67**, 205402 (2003).
[17]W. H. Weber and G. W. Ford, Phys. Rev. B **70**, 125429 (2004).
[18]A. F. Koenderink and A. Polman, Phys. Rev. B **74**, 033402 (2006).
[19]A. Alù and N. Engheta, Phys. Rev. B **74**, 205436 (2006).
[20]V. A. Markel and A. K. Sarychev, Phys. Rev. B **75**, 085246 (2007).
[21]A. A. Govyadinov and V. A. Markel, Phys. Rev. B **78**, 035403 (2008).
[22]S. Campione, S. Steshenko, and F. Capolino, Opt. Express **19**, 18345 (2011).
[23]K. H. Drexhage, J. Lumin. **2**, 693 (1970).
[24]R. R. Chance, A. Prock, and R. Silbey, Adv. Chem. Phys. **37**, 1 (1978).
[25]C. A. Marocico and J. Knoester, Phys. Rev. A **84**, 053824 (2011).
[26]D. V. Orden, Y. Fainman, and V. Lomakin, Opt. Lett. **34**, 422 (2009).
[27]A. B. Evlyukhin and S. I. Bozhevolnyi, Laser Physics Lett. **3**, 396 (2006).
[28]D. Brunazzo, E. Descrovi, and O. J. F. Martin, Opt. Lett. **34**, 1405 (2009).
[29]S. Y. Park and D. Stroud, Phys. Rev. B **69**, 125418 (2004).
[30]M. Meier and A. Wokaun, Opt. Lett. **8**, 581 (1983).
[31]J. D. Jackson, *Classical Electrodynamics* (Wiley, New York, 1998).
[32]L. Novotny and B. Hecht, *Principles of Nano-Optics* (Cambridge University Press, Cambridge, England, 2006).
[33]W. C. Chew, *Waves and Field in Inhomogeneous Media* (Wiley-IEEE Press, New York, 1999).
[34]M. Paulus, P. Gay-Balmaz, and O. J. F. Martin, Phys. Rev. E **62**, 5797 (2000).
[35]Note that $\mathrm{Im}[\overleftrightarrow{\mathbf{G}}^{H}(\mathbf{r}_n,\mathbf{r}_n)]$, which describes the radiation damping of the nth particle, is already taken into account in the polarizability in Eq. (2).
[36]J. Munárriz (private communication).
[37]A. B. Evlyukhin and S. I. Bozhevolnyi, Phys. Rev. B **71**, 134304 (2005).
[38]A. F. Koenderink, R. de Waele, J. C. Prangsma, and A. Polman, Phys. Rev. B **76**, 201403 (2007).
[39]J. J. Mock, R. T. Hill, A. Degiron, S. Zauscher, A. Chilkoti, and D. R. Smith, Nano Lett. **8**, 2245 (2008).